

Mean Field Treatment Of Bose-Einstein Condensate in a Rotating Optical Lattice

MSc. Project Thesis

Vishwanath Shukla
2007PHS0048

Under the Supervision of

Dr. Sankalpa Ghosh



Department Of Physics
Indian Institute of Technology, Delhi
May 2009

April 29, 2009

I dedicate this work to the three F's of my life
Family, Friends, and the joy of Freedom.

Acknowledgements

I would like to thank my advisor Dr. Sankalpa Ghosh for giving me an opportunity to work under his esteemed guidance to explore this novel area of physics. I would also like to take this opportunity to extend my thanks to my friends and hostel buddies for a lively surrounding they provided during the entire course of study. Kanchan, a classmate and a good friend indeed, needs a special mention for the discussions with whom helped clarify several doubts. I'm also grateful to Abhay, a friend of mine, for helping me in running the codes on his PC to get the results on time.

I must mention my parents, sisters, and Namrata for the moral support they provided during the entire project work.

Contents

1	Introduction	1
2	Bose-Einstein condensation	4
2.1	The Phenomenon and its effective theory	4
2.1.1	The Gross-Pitaevskii equation	6
2.2	Condensates under confining potentials	7
2.2.1	Harmonic confinement	7
2.2.2	Dimension reduction	7
2.2.3	Optical confinement	8
2.3	Length and energy scales	9
2.4	Optical lattices	10
2.5	Particles within a periodic potential	11
2.5.1	Single particle treatment	11
2.6	Validity of a mean-field approach in presence of an optical lattice	13
2.7	Ground state properties	13
2.7.1	One- and two-dimensional condensates	13
2.7.2	Approximate analytical solutions	14
2.8	Numerical techniques	15
2.8.1	Dimensionless formalism	16
2.8.2	Imaginary time propagation (ITP) algorithm	17
2.8.3	Discretisation of the condensate wavefunction	18
3	BEC in a rotating optical lattice	19
3.1	Simple rotation of a trapped condensate	19
3.2	Single particle in a periodic potential in a rotating frame . . .	21
3.2.1	Moving lattice	21
3.2.2	Hamiltonian	21
3.2.3	Quasi-angular momentum	23
3.2.4	A toy model - Vortex formation in a box	24
3.3	Two-dimensional rotating optical lattice	25

4	Results	27
4.1	One-dimensional Bose-Einstein condensation	27
4.1.1	Harmonic confinement	27
4.1.2	Optical lattice	30
4.2	Vortex formation in a rotating box	33
4.3	Two-dimensional Bose-Einstein condensation	35
4.3.1	Harmonic confinement	35
4.3.2	Stationary optical lattice	37
4.4	Rotating optical lattice	40
4.4.1	Variation of rotation frequency	41
4.4.2	Variation of the optical lattice potential strength	43
5	Conclusions	45
	bibliography	46

List of Figures

2.1	1D and 2D Bose-Einstein condensates	9
3.1	Rotating optical lattice	20
4.1	Probability density profiles of 1D BEC for differen values of the 1D effective interaction strength	28
4.2	Energy curves for different values of effective interaction strength as function of imaginary time	29
4.3	Density profiles of 1D BEC for different effective strength at constant optical lattice potential	30
4.4	Comparison of density profile with Thomas-Fermi approximation	31
4.5	Density profiles of 1D BEC for different values of optical lattice potential	32
4.6	Probability density profiles for the rotation of a box	33
4.7	Phase distribution for the rotation of a box	33
4.8	Percentage deviation of the ITP solution from its analytical counterpart.	34
4.9	Density profile for the 2D condensate in a harmonic trap in the ideal gas limit	35
4.10	Density profile for the 2D condensate in a harmonic trap at g=100.0	36
4.11	Prob. density profile of a 2D BEC at for different values of optical lattice potential strength	38
4.12	Phase distribution for a 2D condensate in a stationary optical lattice	39
4.13	Prob. density profiles for a 2D BEC in a rot. opt. lattice for the different rotation speeds	41
4.14	Phase distributions for 2D BEC in a rot. opt. lattice for the different rotation speeds	42
4.15	Prob. density profiles for a 2D BEC in a rot. opt. lattice for the different optical lattice strengths	43

4.16 Phase distributions for 2D BEC in a rot. opt. lattice for the
different optical lattice potential strengths 44

Chapter 1

Introduction

In the year 1924, S.N. Bose proposed a proper derivation of the Planck's radiation law treating photons as indistinguishable particles, which obeyed a counting scheme devised by him. Then a year later, in 1925, Einstein generalized this new scheme of counting to include a gas of atoms, whose number is always conserved. Einstein went further, and showed that a gas of atoms obeying this new scheme (*Bose-Einstein statistics*) would suddenly populate the ground state of the system below a certain temperature in observably large numbers. This macroscopic occupation of the ground state is a quantum phase transition, but a one which is purely due to quantum statistical effect, occurring without any inter-particle interaction. This phenomenon was given the name "*Bose-Einstein condensation (BEC)*." The phenomenon is not limited to an ideal system, it occurs in a gas of interacting atoms too. This seemingly strange phase transition waited its verification almost seventy years till 1995, when Bose-Einstein condensation was realized in labs in dilute alkali gases of ^{87}Rb and ^{23}Na atoms cooled in gaseous state down to nano-kelvin and confined in space by an inhomogeneous magnetic field. In fact, BEC in an interacting gas exposes much more richer physics because the interactions may be tuned, the sign as well as strength, at ones will.

The experimental realization of BEC requires the confinement of the bosons in a limited region with the help of some external trapping potentials. BEC of trapped atomic gases like Na , Li etc. are the macroscopic objects which behave according to the laws of quantum mechanics. An interesting situation emerges when the condensate is trapped using some arrangement of laser lights. Such a trap in one dimension can be realized when two coherent counter propagating laser beams interfere. This results in a standing wave with a periodic variation of intensity. The laser light induces an electric dipole moment in the atoms of the condensate, thus modifying their energy.

The trapping configuration can be extended to two- or three-dimension by the use of additional laser beams from different directions. Laser beams in standing wave configuration provide ideal periodic potential for the atoms, these periodic potentials can be regarded as a lattice for the condensate atoms in an analogy with lattices in the real crystalline solids.

The study of Bose-Einstein condensates in optical potentials is multifaced and offers an opportunity to uncover the intriguing properties of coherent matter waves. Optical lattices provide a testing ground for the quantum theory of solids. At the simplest level, it is possible to study the energy band structure of atoms moving in these potentials and to explore experimentally a number of effects that are difficult to observe for electrons in a periodic solid. The interactions among the condensate atoms introduce many novel features in the band structure which can be tackled in the mean-field regime provided there are sufficiently large number of atoms in the vicinity of a single minimum of potential [4]. The most fascinating aspect of this system is that almost all experimental parameters can be controlled with a high degree of precision. The lattice spacing, for example, can be controlled through the wavelength and the angle of the interfering laser beams, the lattice depth is adjustable over a wide range through the intensity of the interfering laser beams. This great control offers the unique possibility of modeling systems that resemble real crystalline lattices, but with lattice constants, barrier heights and interaction parameters that can be varied experimentally. Another very beautiful and important fact is that, even the dimensionality of these systems are controlled, the tight confinement achievable with an optical lattice restricts the motion of the atoms in two or one dimensional region thereby presenting before us another opportunity to study the physics of these one or two dimension systems experimentally. A very interesting variation to the above systems would be to consider the effects of rotation. Under rotation, many new properties of the condensate in an optical lattice may emerge. One may study for an example, how the band structure would get modified by the inclusion of a rotation term in the hamiltonian of the system. Thus, the present study aims at studying and understanding the new physics which may come out by considering the condensates in a rotating optical lattice.

The entire dissertation has been divided into five chapters. The first chapter presents the motivation for the entire work in a very broad manner. Chapter 2 introduces the phenomenon of Bose-Einstein condensation, and then goes on to describe the theory for the interacting condensates, con-

fining potentials and the one- and two-dimensional condensates in sufficient detail. Optical lattice has been explained using simple arguments. Then towards the end the numerical algorithm to study the ground state properties has been discussed at appropriate length. In chapter 3 the theory required to understand the condensate properties in a rotating optical lattice has been put up, an effort has been made to give the essential basic physics involved in the problem. The chapter 4 contains the main results obtained during the entire period of study. Chapter 5 presents the conclusions of the study.

Chapter 2

Bose-Einstein condensation

2.1 The Phenomenon and its effective theory

Non-interacting systems

To elaborate the phenomenon of Bose-Einstein condensation, consider an ideal Bose gas of N particles occupying a volume V . Let N_o and N' be the number of particles in the lowest one-particle state (momentum $\mathbf{p} = 0$) and the number of particles in the higher states ($\mathbf{p} \neq 0$) respectively. Then, following the Bose-Einstein statistics

$$N = \sum_i \frac{1}{e^{\beta(\varepsilon_i - \mu)} - 1}, \quad (2.1)$$

where ε_i is the one-particle energy levels and $\beta = 1/kT$. Also,

$$N = N_o + N' \quad (2.2)$$

with

$$N_o = \frac{1}{e^{-\beta\mu}}, N' = \sum_{i \neq 0} \frac{1}{e^{\beta(\varepsilon_i - \mu)} - 1}, \quad (2.3)$$

where the degeneracy of the lowest energy state $\varepsilon_0 = 0$ has been taken to be unity. Using the density of states expression for the free particles $D(\varepsilon) = 2\pi V(2m/h^2)^{3/2}\varepsilon^{1/2}$

$$\begin{aligned} N' &= 2 \left(\frac{2m}{h^2} \right)^{3/2} \int_0^\infty \frac{\varepsilon^{1/2} d\varepsilon}{e^{\beta(\varepsilon - \mu)} - 1} \\ &= V \left(\frac{2\pi m k T}{h^2} \right)^{3/2} \frac{2}{\sqrt{\pi}} \int_0^\infty \frac{x^{1/2} dx}{e^{x - \beta\mu} - 1} \\ &= V \left(\frac{2\pi m k T}{h^2} \right)^{3/2} F_{3/2}(\alpha), (\alpha = -\beta\mu). \end{aligned} \quad (2.4)$$

The above expression has no contribution from the lowest energy state $\varepsilon = 0$, since the density of states is zero here. This is why N_o was mentioned separately in the Equation (2.2). Moreover, the function $F_{3/2}(\alpha)$ has the form

$$F_{3/2}(\alpha) \equiv \frac{2}{\sqrt{\pi}} \int_0^\infty \frac{x^{1/2} dx}{e^{x+\alpha} - 1} = \sum_{n=1}^{\infty} e^{-n\alpha} / n^{3/2} \quad (2.5)$$

and is defined only in the region $\alpha = -\beta\mu > 0$. So, $F_{3/2}(\alpha)$ is a monotonically decreasing function:

$$F_{3/2}(\alpha) \leq F_{3/2}(0) = \sum_{n=1}^{\infty} n^{-\frac{3}{2}} = 2.612. \quad (2.6)$$

Hence equation (2.4) takes the form,

$$N' < V \left(\frac{2\pi mkT}{h^2} \right)^{\frac{3}{2}} \times 2.612 = N'_{max}(T). \quad (2.7)$$

This condition, Eq. (2.7), signifies that there is an upper limit to the number of particles in the higher states at a given temperature, and as the temperature of the gas is lowered this saturation limit decreases further. When $N'_{max}(T)$ becomes lower than the total number of particles N , the remaining $N - N'_{max}(T)$ particles have no other option but to move to the lowest energy state $\varepsilon = 0$. The temperature at which N'_{max} becomes equal to the total number of particles, defines the critical temperature for the Bose-Einstein condensation to occur. Thus, at low enough temperature a macroscopic fraction of the total population may accumulate in the lowest energy state and form what is known as the Bose-Einstein condensate.

Interacting systems

Following the brief discussion of the phenomenon of Bose-Einstein condensation in an ideal Bose gas, at the next level of complexity is the occurrence of the same in a system of weakly interacting trapped Bose gas. Similar to the ground state of an ideal Bose gas, a dilute weakly interacting Bose gas at low temperature should have nearly all of the particles in the condensate i.e. in the same single-particle state. Thus at absolute zero temperature a condensate of N_o particles behaves as a single macroscopic quantum object and is described by a macroscopic matter wavefunction $\Psi(\mathbf{r}, t)$. The most simplistic picture allows one to write the many body wavefunction a N_o fold product of single particle wavefunction. The condensate represented by $\Psi(\mathbf{r}, t)$ when treated in the mean-field approximation, satisfies a non-linear Schrödinger equation as explained below.

2.1.1 The Gross-Pitaevskii equation

Condensate atoms may be taken to be interacting by means of binary collisions. Since the atoms in the condensate are extremely cold only s -wave scattering is important. The condition that the gas is dilute, the interactions can be modeled by a zero-range potential whose strength is determined by the s -wave scattering length a . In this case each atom feels an additional potential due to mean field of all other atoms present. Potential being proportional to the local atomic density can be included in the Schrödinger equation to account for the atom-atom interactions [5,8]. The discussion so far leads to the following nonlinear Schrödinger equation,

$$i\hbar \frac{\partial \Psi(\mathbf{r}, t)}{\partial t} = \left[-\frac{\hbar^2}{2m} \nabla^2 + V_{ext}(\mathbf{r}) + N_o U_o |\Psi(\mathbf{r}, t)|^2 \right] \Psi(\mathbf{r}, t), \quad (2.8)$$

where

$$\int |\Psi(\mathbf{r}, t)|^2 dr = 1. \quad (2.9)$$

This equation, known as the Gross-Pitaevskii (GP) equation, was derived independently by Gross (1961) and Pitaevskii (1961). This is not the many body wavefunction for N bosons which is a function of N coordinates $(\mathbf{r}_1, \dots, \mathbf{r}_N)$. The coefficient of the non-linear term is given by $U_o = 4\pi\hbar^2 a/m$, where m is the mass of the condensate atom. The condensate atoms repel each other or attract each other depending on whether a is positive or negative. The validity of the above equation is based on the condition that the s -wave scattering length should be much smaller than the average distance between the atoms. Since the Eq.(2.8) was derived under dilute-gas approximation, this fact can be expressed in terms of a dimensionless parameter, $\bar{n}|a|^3$ (where \bar{n} is the average density of the gas), the number of particles in “scattering volume” $|a|^3$. For a dilute or weakly interacting system $\bar{n}|a|^3 \ll 1$ [8].

The wavefunction describing the stationary state of the condensate can be written as

$$\Psi(\mathbf{r}, t) = \psi(\mathbf{r})e^{-i\mu t}, \quad (2.10)$$

where μ is the chemical potential of the condensate system and ψ is the real valued normalized function independent of time. Then, the Gross-Pitaevskii equation takes the form

$$\left(-\frac{\hbar^2}{2m} \nabla^2 + V_{ext}(\mathbf{r}) + N_o U_o |\psi|^2 \right) \psi(\mathbf{r}) = \mu \psi(\mathbf{r}). \quad (2.11)$$

The equation (2.11) is the time-independent Gross-Pitaevskii equation. It must be noted that in the present case eigenvalue is the chemical potential and not the energy per particle as in the case of usual Schrödinger equation. This due to the fact that here one is dealing with a many body state (with majority of particles in the same state) unlike a single particle state. Thus, this is a non-linear Schrödinger equation with non-linearity stemming from the interaction among the atoms treated at mean field level, which is proportional to the particle density $|\psi(\mathbf{r})|^2$.

2.2 Condensates under confining potentials

An important feature of the dilute BEC experiments is the three-dimensional trapping used to spatially confine the atoms. This trapping causes the system to have a finite size. The confinement is most commonly harmonic, formed by magnetic fields. However, other shapes of potential, including gaussian, quartic, step-like, and periodic lattice potentials, can be generated by magnetic and/or optical means.

2.2.1 Harmonic confinement

A three-dimensional harmonic trapping potential can be written as,

$$V_{ext}(\mathbf{r}) = \frac{m}{2}(\omega_x^2 x^2 + \omega_y^2 y^2 + \omega_z^2 z^2) \quad (2.12)$$

where ω_x , ω_y and ω_z are the angular trap frequencies in x , y , and z directions respectively. In the case of a non-interacting ideal gas confined by a 3D harmonic potential, the energy states are the standard harmonic oscillator states. The ground state condensate wavefunction is a gaussian

$$\psi(\mathbf{r}) = \left(\frac{m\bar{\omega}}{\pi\hbar}\right)^{3/4} \exp\left(-\frac{m}{2\hbar}(\omega_x x^2 + \omega_y y^2 + \omega_z z^2)\right) \quad (2.13)$$

with the geometric mean frequency $\bar{\omega} = (\omega_x \omega_y \omega_z)^{1/3}$. In the case of interacting BEC mean field approach is used to obtain the state of the system.

2.2.2 Dimension reduction

In most BEC experiments the atoms are placed in three-dimensional traps which allow them to have a three-dimensional motion. But by deliberately introducing the anisotropy in the trap geometry it is possible to control

the effective dimensionality of the condensate. In this way one- or two-dimensionally confined atomic gas may be produced. In fact, one- and two-dimensional condensates have been realized in elongated and flattened geometries, respectively.

One-dimensional condensates

Consider a cylindrically-symmetric trap geometry $V(\mathbf{r}) = \frac{1}{2}m(\omega_r^2 r^2 + \omega_z^2 z^2)$, where ω_z and ω_r are the longitudinal and radial trap frequencies, respectively. For, $\omega_r \gg \omega_z$, the energy states for the radial direction are very widely spaced as compared to the chemical potential of the system of the system, and so the transverse high-energy modes become ineffective from the point of view of the transverse dynamics. Hence, in this regime longitudinal dynamics, with associated low energy, dominates the system and an effective one-dimensional condensate is formed. In addition to this, the thermal energy $k_B T$ must satisfy the condition $k_B T \ll \hbar \omega_r$ to prevent the thermal excitation of the transverse states.

In effective 1D configuration the radial component of the condensate wavefunction can be approximated by the harmonic oscillator ground state,

$$\psi(r) = (m\omega_r/\hbar\pi)^{1/2} \exp[-m\omega_r r^2/2\hbar], \quad (2.14)$$

with $\int |\psi(r)|^2 2\pi r dr = 1$. The approximation improves with the tighter transverse confinement. Hence, the wavefunction may be expressed as

$$\psi(r, z, t) = \psi_z(z, t)\psi(r). \quad (2.15)$$

Two-dimensional condensates

When $\omega_z \gg \omega_r$, the energy states for the z -direction are very widely spaced and so the condensate may be assumed to always remain in the harmonic oscillator ground state for this direction. Under this situation the condensate takes a highly flattened “pancake-” shape.

2.2.3 Optical confinement

The harmonic confinement discussed above was achieved using some arrangement of magnetic fields in magnetic traps. In the later experiments on the BEC people were able to confine cold bosonic atoms using optical fields, since for cold enough atoms the dipole force offers the possibility of strong confinement. These optical fields can also be manipulated to create a periodic confining potential known as “optical lattice.”

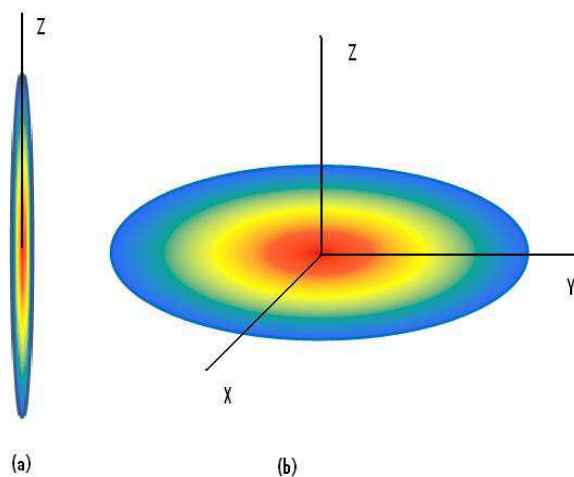


Figure 2.1: (a)1D Cigar-shaped (b)2D Pancake shaped Bose-Einstein condensates

2.3 Length and energy scales

The hierarchy of energy and length scales for trapped gaseous Bose-Einstein condensates simplifies the description of these quantum objects. For each energy E , a length l is defined by the relation $E = \hbar^2/2ml^2$.

In the condensate the separation between atoms is equal to or smaller than the thermal de-Broglie wavelength. The largest length scale involved in the problem is the confinement, either characterized by the size of the trap potential or by the oscillator length $l_{sho} = \sqrt{\hbar/m\omega}$ which is the size of the ground state wavefunction in a harmonic oscillator potential with frequency ω . The atom-atom interactions are described by a mean-field energy $U_o = 4\pi\hbar^2na/m$, where n is the density. The length scale associated with this energy is known as the healing length, and is determined by the balance of the kinetic energy and the mean-field interaction energy.

$$\frac{\hbar^2}{2m\xi^2} = \frac{4\pi\hbar^2na}{m} \quad (2.16)$$

It gives the expression for the healing length as,

$$\xi = (8\pi na)^{-1/2}. \quad (2.17)$$

Healing length represents the distance over which the condensate approaches its bulk density when it is subjected to a local perturbation. In the case of rotating condensates the size of the vortex core is determined by the healing length, ξ .

2.4 Optical lattices

Optical lattices in one-dimension are formed when two laser beams of the same frequency propagating in the opposite directions are superposed. In such a lattice there is a interaction between an induced dipole moment and electric field of the laser. The oscillating electric field of a laser induces an oscillating dipole moment in the atom while at the same time interacts with this dipole moment in order to create trapping potential $V(\mathbf{r})$ for the atoms

$$V(\mathbf{r}) = -d \cdot \mathbf{E}(\mathbf{r}) \propto \alpha(\omega) |\mathbf{E}(\mathbf{r})|^2 \quad (2.18)$$

Here α denotes the polarizability of an atom and $I(\mathbf{r}) \propto |\mathbf{E}(\mathbf{r})|^2$ characterizes the intensity of the laser light field, with $\mathbf{E}(\mathbf{r})$ as its electric amplitude at position \mathbf{r} [11]. Assuming that both beam are linearly polarized with the electric field vector along the z-axis, the resultant field is

$$\mathbf{E}_z = \mathbf{E}_o \cos(qx - \omega t) + \mathbf{E}_o \cos(-qx - \omega t) = 2\mathbf{E}_o \cos(qx) \cos(\omega t) \quad (2.19)$$

Thus the potential is proportional to the square of the time-varying electric field (averaged over one time period), which is given by

$$\langle \mathbf{E}_z^2 \rangle_t = 2\mathbf{E}_o^2 \cos^2(qx). \quad (2.20)$$

Thus the potential created is periodic in x , with a period equal to π/q [4]. In terms of the wavelength of laser light $\lambda = 2\pi/q$, the period is $\lambda/2$. The above potential can be written as

$$V_{ol}(x) = V_o \cos^2\left(\frac{\pi x}{d}\right) \quad (2.21)$$

where $d = \pi/q = \lambda/2$ is the period and V_o is a constant.

2.5 Particles within a periodic potential

To have a better understanding of atoms in optical lattices it is important to review quantum mechanical motion of a particle in a the simple periodic potential. A periodic potential V in one dimension at point x has the property

$$V(x) = V(x + d) \quad (2.22)$$

denoting its translational property, i.e. the potential value repeats itself after any number of crystal translation displacements d . In the present case, atoms are confined in a periodic potential which is created by a standing light wave. Thus, the lattice potential may be taken to be either

$$V_{ol}(x) = \cos^2\left(\frac{\pi x}{d}\right) \quad (2.23)$$

or

$$V_{ol}(x) = \sin^2\left(\frac{\pi x}{d}\right) \quad (2.24)$$

where V_{ol} denotes optical lattice potential.

2.5.1 Single particle treatment

Particles in optical lattices follow the same basic physics, as electrons do in crystal lattices in solids. When a periodic potential is introduced in the system, it breaks the continuous translational symmetry of the system, and the wavefunction describing the particle cease to remain the eigenstates of the momentum operator. For definiteness and simplicity, one-dimensional system can be taken up which illustrates the phenomenon. Behavior of the particle in this potential is governed by the Schrödinger equation

$$\left[-\frac{\hbar^2}{2m} \frac{\partial^2}{\partial x^2} + V_{ol}(x) \right] \psi(x) = E\psi(x), \quad (2.25)$$

where $V_{ol}(x) \equiv$ optical lattice potential seen by the particle, $\psi(x) \equiv$ wavefunction for the particle in the system and $E \equiv$ energy of the particle.

Now in the present system Hamiltonian, H , is invariant under translation by a lattice spacing d , which is due to the periodic nature of the potential. Mathematically, the eigenfunctions of the Hamiltonian are also the eigen functions of the discrete translation operator T_d (a translation operator translates the entire system by one lattice spacing). Thus, H and T_d commute with each other

$$[H, T_d] = 0. \quad (2.26)$$

Now suppose there are N number of lattice sites, then the application of periodic boundary condition, $\psi(x + Nd) = \psi(x)$, which implies

$$T_d^N \psi(x) = \psi(x). \quad (2.27)$$

Therefore the eigenvalues are of the form $e^{i2\pi n/N}$, where n is an integer. Thus,

$$\psi(x + d) = e^{i2\pi n/N} \psi(x) = e^{ikd} \psi(x), \quad (2.28)$$

where $k = \frac{2\pi n}{Nd}$.

From the above discussion it can be seen that the function $u(x) = \psi(x)e^{-ikx}$ is periodic in space with the same period as the lattice potential. So the eigenfunctions of the Schrödinger equation have the form of a plane wave e^{ikx} modulated by a function having the same periodicity as that of the lattice or

$$\psi_k(x) = u_k e^{ikx}, \quad (2.29)$$

where u_k satisfies the condition $u_k(x) = u_k(x + d)$ and k is the wave number and can be used to label the wavefunctions.

For a given k there are many different states characterized by the band in which it lies, so in general the stationary state of the wavefunction is written by putting an additional subscript ν , denoting the band index, to the wave function. The above treatment goes by the name of Bloch's theorem in the context of the electron band theory. The wave functions in three dimension take the following form

$$\psi_{k,\nu}(\mathbf{r}) = u_{k,\nu}(\mathbf{r}) e^{i\mathbf{k}\cdot\mathbf{r}}, \quad (2.30)$$

where \mathbf{k} is the wave vector. The quantity $\hbar\mathbf{k}$ is referred to as the *quasi-momentum*, and so $\psi_{k,\nu}$ is the *quasi-momentum* eigenstate of the system.

When the Bloch functions Eq.(3.9) are expanded in the momentum basis, the only momenta contributing to the sum is then given by

$$\psi_{k,\nu}(x) = \int \frac{dq}{\sqrt{2\pi}} e^{iqx} \psi_{k,\nu}(q) = \sum_{j=-\infty}^{j=\infty} c_{j,\nu} \frac{e^{i(k+2\pi j/d)x}}{\sqrt{2\pi}}, \quad (2.31)$$

where the expansion coefficients are given by

$$c_{j,\nu} = \int dx \frac{e^{-i(k+2\pi j/d)x}}{\sqrt{2\pi}} \psi_{k,\nu}(x). \quad (2.32)$$

2.6 Validity of a mean-field approach in presence of an optical lattice

For the mean-field approach to remain valid for studying the condensate properties in an optical lattice, the strength of the later must not be too high to destroy the phase coherence property of the condensate. If the optical lattice is too deep, it makes the tunneling of the atoms through the optical barrier difficult and there by disrupting the coherence property in an extreme limit.

2.7 Ground state properties

The wavefunction $\psi(\mathbf{r})$ used to describe the various ground state properties of a condensate at zero-temperature is determined by the solution to the time-independent Gross-Pitaevskii equation, Eqn.(2.11). This section briefly introduces the GP equation in one- and two-dimensions, and towards the end its approximate analytical solutions in the limiting cases have been discussed.

2.7.1 One- and two-dimensional condensates

Keeping in mind the discussion of the section (2.2.2) the condensate properties may be continued to be described under mean-field approach by the Gross-Pitaevskii equation, with suitable modification in the interaction energy term. The wavefunction for the one-dimensional condensate given by the equation (2.15), with radial part of the wavefunction being a harmonic oscillator ground state wavefunction. When this equation is substituted in the Gross-Pitaevskii equation, Eqn.(2.8), and the entire equation is multiplied by $\psi^*(r)$ and is integrated with respect to r we get

$$i\hbar \frac{\partial \Psi(x, t)}{t} = \left[-\frac{\hbar^2}{2m} \frac{\partial^2}{\partial x^2} + V_{ext}(x) + g_{1d} |\Psi(x, t)|^2 \right] \Psi(x, t) \quad (2.33)$$

with

$$\int |\Psi(x, t)|^2 dx = 1, \quad (2.34)$$

where g_{1d} is the effective interaction strength in one-dimension. The above equation is the Gross-Pitaevskii equation for describing the one dimensional condensate properties. Similarly, the Gross-Pitaevskii equation for the two-dimensional condensates takes the form

$$i\hbar \frac{\partial \Psi(x, y, t)}{\partial t} = \left[-\frac{\hbar^2}{2m} \left(\frac{\partial^2}{\partial x^2} + \frac{\partial^2}{\partial y^2} \right) + V_{ext}(x, y) + g_{2d} |\Psi(x, y, t)|^2 \right] \Psi(x, y, t) \quad (2.35)$$

with

$$\int |\Psi(x, y, t)|^2 dx dy = 1, \quad (2.36)$$

where g_{2d} is the effective interaction strength in two-dimension.

2.7.2 Approximate analytical solutions

In general, this non-linear equation must be solved numerically except in few limiting cases where it lends an easy analytical solution. These limiting cases appear when there are either very few or many atoms in the condensate confined to a limited region of space.

Ideal-gas limit

In the limit of very weak interactions $N_o U_o \ll \hbar \omega_{x,y,z}$, i.e. $N_o \rightarrow 1$ one can neglect the interaction term in the Eqn.(2.11). Then the condensate wavefunction is simply the ground state of the harmonic oscillator, which gives a density for N_o of

$$|\psi(\mathbf{r})|^2 = N_o (\omega_x \omega_y \omega_z)^{1/2} \left(\frac{m}{\pi \hbar} \right)^{3/2} \exp\left(-\frac{m}{2\hbar} (\omega_x x^2 + \omega_y y^2 + \omega_z z^2)\right). \quad (2.37)$$

Thomas-Fermi Limit

In the limit of strong interactions $N_o U_o \gg \hbar \omega_{x,y,z}$, i.e. $N_o \rightarrow \infty$ the determination of the trapped condensate wavefunction is simplified by neglecting the kinetic energy which is now much smaller than the interaction term. In this limit, known as the Thomas-Fermi limit, the ground state solution becomes

$$\psi_{TF}(\mathbf{r}) = \sqrt{\frac{1}{N_o U_o} [\mu_{TF} - V_{ext}(\mathbf{r})]}. \quad (2.38)$$

When the condensate is confined using an isotropic harmonic trap, $V_{ext}(\mathbf{r} = \frac{1}{2} m \omega r^2)$, Eqn.(2.38) takes the form

$$\psi_{TF}(\mathbf{r}) = \sqrt{\frac{1}{N_o U_o} [\mu_{TF} - \frac{1}{2} m \omega r^2]}. \quad (2.39)$$

The Thomas-Fermi radius is determined by solving for r in the expression $V(\mathbf{r}) = \mu_{TF}$, which gives

$$r_{TF} = \sqrt{\frac{2\mu_{TF}}{m\omega}}. \quad (2.40)$$

The chemical potential for the system in such a situation can be determined from the normalization condition

$$4\pi \int_0^{r_{TF}} r^2 dr |\psi_{TF}|^2 = 1. \quad (2.41)$$

This gives the chemical potential in the Thomas-Fermi limit as

$$\mu_{TF} = \frac{\hbar\omega}{2} [15N_o(\frac{a}{l_{sho}})]^{2/5} \quad (2.42)$$

where l_{sho} is the size of the harmonic oscillator ground state. The condensate in this limit can be thought of as “filling in” the bottom of the trapping potential up to a “height” of the chemical potential μ_{TF} . Thus, the size of the condensate in the Thomas-Fermi limit is given by

$$r_{TF} = l_{sho}(\frac{15N_o a}{l_{sho}})^{1/5}. \quad (2.43)$$

The Thomas-Fermi approximation becomes increasingly accurate as the number of atoms in the condensate increases and the mean-field energy of the condensate dominates the kinetic energy.

2.8 Numerical techniques

This section deals with the computational techniques which were used during course of study. This includes the numerical methods which were used to solve the Gross-Pitaevskii equation, both in one- and two-dimensions, to obtain the ground state solution. The algorithms were implemented in the FORTRAN-95 and the data so obtained was plotted in the MATLAB. The Gross-Pitaevskii equation is non-linear Schrödinger equation, a non-linear partial differential equation. There are no exact analytical solution of this equation except under few special cases (e.g. Thomas-Fermi limit). The ground state solution of the equations (2.33) and (2.35) were obtained using a technique called imaginary time propagation.

2.8.1 Dimensionless formalism

An appropriate choice of dimensionless quantities minimizes the number of adjustable parameters to few in the numerical simulation of a problem in hand. Also, it scales the various physical quantities involved, in units of those which are the characteristics of the system so that one does not have to deal with very large or small numbers unnecessarily. The Eqn.(2.8) may be transformed into a dimensionless form using the following transformed variables

$\tilde{t} = \omega_o t$, $\tilde{\mathbf{r}} = \mathbf{r}/l_{sho}$, $\tilde{\Psi}(\tilde{\mathbf{r}}, t) = l_{sho}^{3/2} \Psi(\mathbf{r}, t)$ where $\omega_o = \min(\omega_x, \omega_y, \omega_z)$ and $l_{sho} = \sqrt{\hbar/m\omega_o}$ is the length of the harmonic oscillator ground state. Thus, length and time are in units of l_{sho} and ω_o^{-1} . The dimensionless GP equation in three-dimension takes the form, after doing away with $\tilde{}$

$$i \frac{\partial \Psi(\mathbf{r}, t)}{\partial t} = \left[-\frac{1}{2} \nabla^2 + V_{ext}(\mathbf{r}) + g |\Psi(\mathbf{r}, t)|^2 \right] \Psi(\mathbf{r}, t), \quad (2.44)$$

where $V_{ext}(\mathbf{r}) = \frac{1}{2}(\gamma_x x^2 + \gamma_y y^2 + \gamma_z z^2)$, $\gamma_x = \frac{\omega_x}{\omega_o}$, $\gamma_y = \frac{\omega_y}{\omega_o}$, $\gamma_z = \frac{\omega_z}{\omega_o}$, and $g = 4\pi N_o/l_{sho}$.

1D GP equation

The dimensionless Gross-Pitaevskii equation for the one-dimensional Bose-Einstein condensate may be written as

$$i \frac{\partial \Psi(x, t)}{\partial t} = \left[-\frac{1}{2} \frac{\partial^2}{\partial x^2} + \frac{1}{2} x^2 + g_{1d} |\Psi(x, t)|^2 \right] \Psi(x, t), \quad (2.45)$$

where g_{1d} is the effective interaction strength in one-dimension. The energy functional, in the dimensionless form, to be used for calculating the ground state energy is given by

$$E(\psi) = \int \left[\frac{1}{2} |\nabla \psi|^2 + V_{ext}(x) + \frac{1}{2} g_{1d} |\psi|^4 \right] dx. \quad (2.46)$$

2D GP equation

Similarly, the dimensionless form of GP equation for the two-dimensional condensate is

$$i \frac{\partial \Psi(x, y, t)}{\partial t} = \left[-\frac{1}{2} \left(\frac{\partial^2}{\partial x^2} + \frac{\partial^2}{\partial y^2} \right) + V_{ext}(x, y) + g_{2d} |\Psi(x, y, t)|^2 \right] \Psi(x, y, t), \quad (2.47)$$

where $V_{ext}(x, y) = \frac{1}{2}(x^2 + \gamma_y y^2)$ with $\omega_o = \omega_x$ and g_{2d} is the effective coupling constant for the two dimensional condensate [10]. The corresponding energy functional in the dimensionless for the two-dimension condensate is given by

$$E(\psi) = \int \left[\frac{1}{2} |\nabla \psi|^2 + \frac{1}{2} (x^2 + \gamma_y y^2) + g_{2d} |\psi|^4 \right] dx dy. \quad (2.48)$$

2.8.2 Imaginary time propagation (ITP) algorithm

One method which is both reliable and easily-implemented for computing the ground state solution of the GP equation is the imaginary time propagation (ITP) algorithm [9]. To see how this works, consider the wavefunction as a superposition of eigenstates $\phi_i(\mathbf{r})$ with time-dependent amplitudes $c_i(t)$ and eigen energies $E_i(t)$, i.e.

$$\Psi(\mathbf{r}, t) = \sum_i c_i(t) \phi_i(\mathbf{r}). \quad (2.49)$$

Now when one sets $t \rightarrow -i\tau$ in the unitary evolution operator so that the solution in imaginary time is given by

$$\Psi(\mathbf{r}, \tau) = e^{-\tau H/\hbar} \Psi(\mathbf{r}, 0). \quad (2.50)$$

The above equation can be rewritten as

$$\Psi(\mathbf{r}, \tau) = e^{-\tau H/\hbar} \sum_i c_i(0) \phi_i(\mathbf{r}). \quad (2.51)$$

The above time evolution shows that different eigenstates in the expansion decay exponentially at different rates depending upon their eigen energies. The important fact here is that the lowest energy state i.e. the ground state has the smallest decay constant, and it decays away the slowest.

The initial guess $\Psi(\mathbf{r}, 0)$ for the ground state will contain some finite contribution from the excited states in the expansion. This contribution from the excited states in the initial guess will decay away faster than the ground state part of the expansion. After a sufficiently long time interval T_o , the solution is then

$$\Psi(\mathbf{r}, T_o) \approx c_o e^{-T_o E_o/\hbar} \phi_o(\mathbf{r}). \quad (2.52)$$

Also, while implementing the procedure the wave function must be re-normalized periodically in time due to decaying norm of the solution. Specially when solving the non-linear GP equation one must re-normalize the wave function at each step, since the Hamiltonian depends on the density $|\Psi(\mathbf{r}, t)|^2$ of the solution.

2.8.3 Discretisation of the condensate wavefunction

To numerically determine the ground state solution of the Gross-Pitaevskii equation it is necessary to discretize the condensate wavefunction. This has been done on an equi-spaced position basis. The wavefunction $\Psi(\mathbf{r}, t)$ is represented in one dimension by Ψ_i corresponding to position (x_i) , and in two-dimensions by $\Psi_{i,j}$ on positions (x_i, y_j) . A similar discretization has been performed in the time domain too, at time t the wavefunction is denoted by Ψ^k . The difference in the position between two grid points has been denoted by Δx , Δy along x- and y-directions respectively. The size of time step is represented by Δt in the discretized equations. Thus, the dimensionless GP equation, after incorporating ITP algorithm and using Euler discretization scheme, in one dimension may be written as

$$-\frac{[\Psi_i^{k+1} - \Psi_i^k]}{\Delta t} = -\frac{1}{2} \left(\frac{\Psi_{i+1}^k - 2\Psi_i^k + \Psi_{i-1}^k}{(\Delta x)^2} \right) + \frac{1}{2} x_i^2 \Psi_i^k + g_{1d} |\Psi_i^k|^2 \Psi_i^k. \quad (2.53)$$

Similarly, the dimensionless GP equation, after incorporating ITP algorithm, in two-dimensions may be written as

$$-\frac{[\Psi_{i,j}^{k+1} - \Psi_{i,j}^k]}{\Delta t} = -\frac{1}{2} \left(\frac{\Psi_{i+1,j}^k - 2\Psi_{i,j}^k + \Psi_{i-1,j}^k}{(\Delta x)^2} \right) - \frac{1}{2} \left(\frac{\Psi_{i,j+1}^k - 2\Psi_{i,j}^k + \Psi_{i,j-1}^k}{(\Delta y)^2} \right) + \frac{1}{2} (x_i^2 + y_j^2) \Psi_{i,j}^k + g_{2d} |\Psi_{i,j}^k|^2 \Psi_{i,j}^k. \quad (2.54)$$

Chapter 3

BEC in a rotating optical lattice

The main aim of this study is to understand the behavior of the Bose-Einstein condensates in a rotating optical lattice. The case of trapped rotating interacting condensate has been a subject of great research, and the new variation to this problem is inclusion of the optical lattice potential. An optical lattice is a very versatile tool which offers us an opportunity to manipulate our condensate in a variety of ways. One such scheme is the creation of a rotating optical lattice along with the condensate confinement. This unique feature of it, along with many others as mentioned in the introduction, makes the experimental study of the response of the condensate very versatile and interesting. Various groups have already carried out such experiments, among them are Tung *et al.*, at JILA [15] and Williams *et al.* [16], at University of Oxford, to name a few. The Oxford group has devised the following interesting scheme to generate a rotating optical lattice. Two parallel beams were allowed to be incident on a lens and these formed a 1D optical lattice in the focal plane of the lens where they intersect. The cylindrical symmetry of such an arrangement allowed them to achieve a rotating lattice upon rotation of the parallel beams incident on a lens. And finally two orthogonal 1D lattices were combined to form a 2D rotating lattice as shown in the figure (3).

3.1 Simple rotation of a trapped condensate

Before taking up the issue of condensates in a rotating optical lattice, it is worth while to recall the response of a trapped condensate to rotation in the absence of former. Being a complex number the condensate wavefunction may be written as $\Psi(\mathbf{r}) = |\Psi(\mathbf{r})|e^{-i\phi(\mathbf{r})}$, and the superfluid velocity can be

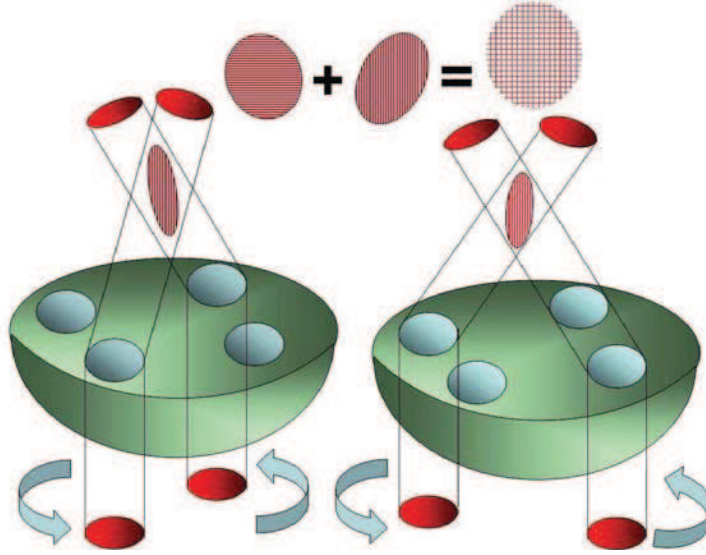


Figure 3.1: Two orthogonal standing wave intensity patterns in the focal plane of a lens combine to form a 2D lattice. The axial symmetry of the system allows rotation of the lattice to be realized.

then inferred from the particle current density

$$\mathbf{j} = \frac{\hbar}{2mi}(\Psi^*\nabla\Psi - \Psi\nabla\Psi^*) = |\Psi|^2\frac{\hbar}{m}\nabla\phi. \quad (3.1)$$

Since, $\mathbf{j} = n\mathbf{v}$ the velocity in terms of the condensate phase is

$$\mathbf{v} = \frac{\hbar}{m}\nabla\phi(\mathbf{r}). \quad (3.2)$$

Thus, it can be seen that \mathbf{v} is irrotational, $\nabla\times\mathbf{v} = 0$, everywhere except at the points where phase $\phi(\mathbf{r})$ has a singularity. Furthermore, as a consequence of single-valuedness of the wavefunction, the change in phase around any closed path turns out to be an integer multiple of 2π ,

$$\oint_s d\mathbf{l}\cdot\mathbf{v}(\mathbf{r}) = \oint_s \frac{\hbar}{m}\nabla\phi\cdot d\mathbf{l} = 2\pi q\frac{\hbar}{m}, \quad (3.3)$$

i.e. circulation in BEC is quantized in units of $2\pi\hbar/m$. In order to cancel the effect of diverging velocity, the condensate density must vanish at singularity. The vanishing structure is referred to as a vortex. So, the condensate

responds to rotation by forming vortices in the density profile at the phase singularities and remains irrotational in the remaining region.

3.2 Single particle in a periodic potential in a rotating frame

Study of a single particle in a rotating optical lattice may be prove to be helpful in understanding the basic physics involved in the condensate's response to the same. So, in this section too as in section (2.5), first, a study has been done in the context of a single particle starting from the hamiltonian which describes the system in the rotated frame of reference. Thereafter, the concept of quasi-angular momentum, which emerges in the treatment of rotating N-site sinusoidal ring lattice, has been discussed.

3.2.1 Moving lattice

Instead of considering the effect of rotation of an optical lattice first, it would be interesting to observe the effect of linear motion. Suppose the lattice is moving at a uniform velocity \mathbf{v} with respect to a stationary frame, then the Hamiltonian in the frame attached to the lattice is given by

$$H = H_o - \mathbf{p} \cdot \mathbf{v}, \quad (3.4)$$

where H_o is the Hamiltonian in the stationary frame. Considering an eigenfunction $\psi_k(x)$ of H_o and assuming $\mathbf{p} \cdot \mathbf{v}$ to be small, the application of first-order perturbation theory gives

$$E_k = \int dx \psi_k^* (H_o - \mathbf{p} \cdot \mathbf{v}) \psi_k = E_k^o - v \int dx \psi_{k'}^*(p) \psi_k, \quad (3.5)$$

which is the expression for the ground state energy under the new situation. So if the quantity $\int dx \psi_{k'}^*(p) \psi_k$, average momentum, is positive then a translating lattice has a lower ground state energy as compared to the stationary lattice.

3.2.2 Hamiltonian

The Hamiltonian for a single particle in a stationary optical lattice is given by

$$H_o = -\frac{\hbar^2}{2m} \nabla^2 + V_{ol}(x, y). \quad (3.6)$$

When rotation is considered, the time dependence in rotating potentials can be avoided by making a coordinate transformation to a coordinate system rotating with the same angular velocity as the potential. Now the Hamiltonian is expressed using rotating frame coordinates [13, 14]. Consider the particle to be rotating about the z-axis with an angular velocity, ω in the stationary frame.

The position vector of the particle is $\mathbf{r}(\equiv \mathbf{r}_o)$ and the velocity is $v_o = \omega \times \mathbf{r}$, thus the angular momentum in the stationary frame is

$$\mathbf{L}_o = m(\mathbf{r} \times \mathbf{v}_o) = \mathbf{r} \times \mathbf{p}_o \quad (3.7)$$

The Lagrangian in the stationary frame is

$$\mathcal{L}_o = \frac{1}{2}mv_o^2 = H_o, \quad (3.8)$$

where H_o is the Hamiltonian for the system in the stationary coordinate system.

Now the velocity of the particle in a frame which is rotating with an angular velocity Ω with respect to stationary frame is given by

$$\mathbf{v} = \mathbf{v}_o - \Omega \times \mathbf{r}. \quad (3.9)$$

Thus, the Lagrangian in the rotating frame coordinates can be written as

$$\begin{aligned} \mathcal{L} &= \mathcal{L}_o = \frac{1}{2}mv_o^2 = \frac{1}{2}m(\mathbf{v} + \Omega \times \mathbf{r})^2 \\ &= \frac{1}{2}mv^2 + m\mathbf{v} \cdot (\Omega \times \mathbf{r}) + \frac{1}{2}m(\Omega \times \mathbf{r})^2. \end{aligned} \quad (3.10)$$

The conjugate momenta can be obtained as

$$d\mathcal{L} = m\mathbf{v} \cdot d\mathbf{v} + m(\Omega \times \mathbf{r}) \cdot d\mathbf{v} + m\mathbf{v} \cdot (\Omega \times d\mathbf{r}) + m(\Omega \times d\mathbf{r}) \cdot (\Omega \times \mathbf{r}), \quad (3.11)$$

$$\mathbf{p} = \frac{\partial \mathcal{L}}{\partial \mathbf{v}} = m\mathbf{v} + m(\Omega \times \mathbf{r}) = m\mathbf{v}_o = \mathbf{p}_o. \quad (3.12)$$

$$\mathbf{L} = \mathbf{r} \times \mathbf{p} = \mathbf{r} \times \mathbf{p}_o. \quad (3.13)$$

The Hamiltonian in the rotating frame is then given by

$$\begin{aligned}
H &= \mathbf{p} \cdot \mathbf{v} - \mathcal{L} = mv^2 + m\mathbf{v} \cdot (\Omega \times \mathbf{r}) - \frac{1}{2}mv^2 - m\mathbf{v} \cdot (\Omega \times \mathbf{r}) - \frac{1}{2}m(\Omega \times \mathbf{r})^2 \\
&= \frac{1}{2}mv^2 - \frac{1}{2}m(\Omega \times \mathbf{r})^2 \\
&= \frac{1}{2}m(\mathbf{v}_o - \Omega \times \mathbf{r})^2 - \frac{1}{2}m(\Omega \times \mathbf{r})^2 \\
&= \frac{1}{2}mv_o^2 - \Omega \cdot (\mathbf{r} \times p_o) \\
&= \frac{p_o^2}{2m} - m\Omega \cdot \mathbf{L} \\
&= H_o - \Omega \cdot \mathbf{L}.
\end{aligned} \tag{3.14}$$

3.2.3 Quasi-angular momentum

In the present section an attempt has been made to understand and present the consequences of having such a hamiltonian, Eqn. (3.14), for the system following the work done by Rajiv Bhat *et al.*[12].

A moving N-site linear optical lattice with periodic boundary conditions is equivalent to a rotating, N-site ring lattice. This analogy can be made explicit by considering the Hamiltonian for the particle in a moving, one dimensional, sinusoidal N-site lattice. The hamiltonian in the co-moving frame, Eqn. (3.4) is given by

$$H = -\frac{\hbar^2}{2m} \frac{\partial^2}{\partial x^2} + V_o \cos^2(qx) - \frac{v\hbar}{i} \frac{\partial}{\partial x} \tag{3.15}$$

where v is the velocity of the lattice and $q = \pi/d$. Under periodic boundary conditions

$$\psi(x + Nd) = \psi(x). \tag{3.16}$$

Where as, the Hamiltonian of a rotating sinusoidal N-site ring lattice in the rotating frame is given by

$$H = -\frac{\hbar^2}{2m} \frac{1}{R^2} \frac{\partial^2}{\partial \phi^2} + V_o \cos^2(N\phi/2) - \Omega \frac{\hbar}{i} \frac{\partial}{\partial \phi}, \tag{3.17}$$

where Ω is the rotation frequency, R is the radius of the ring, and $-i\hbar \frac{\partial}{\partial \phi}$ is the angular momentum operator, L_z . The two hamiltonians, Eq.(3.15) and Eq.(3.17), are identical if one considers the transformation $x = \phi Nd/2\pi$ and identifies $Nd/2\pi$ with R and v/R with Ω .

The fact that the above Hamiltonians are exactly identical, ensures that all the properties of one-dimensional systems with a discrete translational invariance are inherited to the ring systems with a discrete rotational invariance. Thus if,

$$\psi_j(\rho, \phi) = e^{i j \phi} R_j(\rho) \quad (3.18)$$

where $R_j(\rho)$ is a radial function and j is an integer, are two-dimensional free space solutions in polar coordinates. Then analogous to the linear lattice, in the ring system in the presence of a potential that breaks the rotational symmetry, the eigenstates of the Hamiltonian, Eq.(3.17), are linear combinations of the above free space solutions, Eq.(3.18). For the potential with a discrete N -fold rotational symmetry, the eigenstates can be written as

$$\psi_m(\phi, \rho) = \sum_{j=-\infty}^{\infty} a_j e^{i(Nj+m)\phi} R_j(\rho). \quad (3.19)$$

Thus ψ_m is an eigenstate with eigenvalue $e^{-i2\pi m/N}$ of the discrete rotational operator $R_{2\pi/N}$ that rotates the system by an angle $2\pi/N$; and plays a role analogous to the discrete translational operator, T_d . The analogy is complete when it is noted that the eigenstates are linear combination of the angular momentum eigenstates, in which case the number $\hbar m$ is referred as the quasi-angular momentum of the state, $\psi_m(\rho, \phi)$.

3.2.4 A toy model - Vortex formation in a box

Consider a single particle in a 2×2 lattice bounded by a box rotating about its center. The single-particle Hamiltonian for the system in the rotating frame is,

$$H = -\frac{\hbar^2}{2m} \left(\frac{\partial^2}{\partial x^2} + \frac{\partial^2}{\partial y^2} \right) + V_{box}(x, y) + i\hbar\Omega \left(x \frac{\partial}{\partial y} - y \frac{\partial}{\partial x} \right), \quad (3.20)$$

where V_{box} is the potential corresponding to the box with very high potential walls, and Ω is the frequency with which box is rotating. The Schrödinger equation describing the above system follows from the Eqn.(3.20), and is

$$i\hbar \frac{\partial \Psi}{\partial t} = \left[-\frac{\hbar^2}{2m} \left(\frac{\partial^2}{\partial x^2} + \frac{\partial^2}{\partial y^2} \right) + i\hbar\Omega \left(x \frac{\partial}{\partial y} - y \frac{\partial}{\partial x} \right) \right] \Psi \quad (3.21)$$

The ground state of the above equation (3.21) may be obtained using ITP algorithm, discussed in section (2.8.2). The dimensionless form is obtained

by dividing the entire equation by $E_R = \pi^2 \hbar^2 / 2m(L/2)^2$, where L is the length of the box,

$$i \frac{\partial \Psi}{\partial t} = \left[- \left(\frac{\partial^2}{\partial x^2} + \frac{\partial^2}{\partial y^2} \right) + i 2\pi\alpha \left(x \frac{\partial}{\partial y} - y \frac{\partial}{\partial x} \right) \right] \Psi, \quad (3.22)$$

with $t \rightarrow \frac{t}{mL^2/2\hbar}$, $x \rightarrow \frac{x}{L/2}$, $y \rightarrow \frac{y}{L/2}$, and $\Omega \rightarrow \frac{4\pi\hbar\alpha}{mL^2}$. The initial guess solution for the ITP algorithm may taken to be based on the ground state solution of the non-rotating box potential,

$$\psi(x, y) = \cos\left(\frac{\pi x}{2} + b\right) \cos\left(\frac{\pi y}{2} + b\right), \quad (3.23)$$

where b is a parameter which represents the deviation.

3.3 Two-dimensional rotating optical lattice

In this section, the study of the ground state properties of Bose-Einstein condensate in a two-dimensional rotating optical lattice has been taken up. The condensate still can be described under the mean-field approximation, the GP equation, provided the optical lattice strength is not too strong. The treatment also assumes that, initially the condensate is in the ground state and is confined by a harmonic potential, and then a rotating optical lattice potential is switched on. Then, the Gross-Pitaevskii equation describing the above system is

$$i\hbar \frac{\partial \Psi(x, y, t)}{\partial t} = \left[- \frac{\hbar^2}{2m} \left(\frac{\partial^2}{\partial x^2} + \frac{\partial^2}{\partial y^2} \right) + V_{ext}(x, y) + V_{ol}(x, y) - \Omega L_z + g_{2d} |\Psi(x, y, t)|^2 \right] \Psi(x, y, t), \quad (3.24)$$

where $V_{ext}(x, y) = \frac{1}{2}m\omega^2(x^2 + y^2)$, V_{ol} is the optical lattice strength, Ω is the optical lattice rotation frequency, L_z is the z-component of the angular momentum, and m, ω are the mass of the condensate atoms and the harmonic trap frequency respectively. The energy in the rotating frame is given by the expression

$$E = E_o - \Omega.L, \quad (3.25)$$

where E_o is the energy in the stationary frame.

Since, an analytical solution of this equation is not possible, so the ground state solution has been computed numerically by employing the ITP algorithm. The discussion for the numerical computation can be simplified by

adopting a energy scale, $\hbar\omega$, which is the kinetic energy corresponding to the length scale l_{sho} (length of the ground state wavefunction in a harmonic oscillator potential). The dimensionless form of the Eqn.(3.24) is,

$$i\frac{\partial\Psi(x, y, t)}{\partial t} = \left[-\frac{1}{2}\left(\frac{\partial^2}{\partial x^2} + \frac{\partial^2}{\partial y^2}\right) + \frac{1}{2}(x^2 + y^2) + v_{ol}\left(\sin^2\left(\frac{\pi x}{d}\right) + \sin^2\left(\frac{\pi y}{d}\right)\right) - i\alpha\left(x\frac{\partial}{\partial y} - y\frac{\partial}{\partial x}\right) + g|\Psi(x, y, t)|^2\right]\Psi(x, y, t), \quad (3.26)$$

where the units for length, time, and energy are $\sqrt{\hbar/m\omega}$, ω^{-1} , and $\hbar\omega$ respectively. v_{ol} is optical lattice energy in terms of harmonic trap energy, i.e. $v_{ol} = V_{ol}/\hbar\omega$, α is the rotation frequency of the lattice in units of the harmonic trap frequency ($\alpha = \Omega/\omega$), d is the lattice constant in terms of l_{sho} , and g is the dimensionless parameter characterizing the interaction strength of the condensate atoms in two-dimensions. The dimensionless form for the energy expression following Eqn.(3.25) is

$$E = E_o - \alpha Re[\psi^* L_z \psi], \quad (3.27)$$

where E_o is the energy in the stationary frame in units of $\hbar\omega$.

Chapter 4

Results

Results

In this chapter, the results of all the numerical simulations and the important plots pertaining to the problem under study have been presented. The results have been presented in the order of complexity of the numerical scheme for the solutions to tackle the problems, which was followed to achieve the final aim of the study, i.e. the ground state properties of a Bose-Einstein condensate confined in a rotating optical lattice.

4.1 One-dimensional Bose-Einstein condensation

The numerical study of a one-dimensional problem is relatively easier and it requires a less computational time as compared to their two-and three-dimensional analogues. So, the one-dimensional Bose-Einstein condensation was taken up first and its ground state properties were studied under harmonic and optical lattice potential confinement.

4.1.1 Harmonic confinement

The details on it have been given in the section (2.2.1), and section (2.7.1). The ground state solution of the GP equation, Eq.(2.45), and its comparison with Thomas-fermi solution is being presented here.

The initial guess in the ITP algorithm to obtain the ground state solution of Eq.(2.45) has been taken to be the ground state of the harmonic oscillator

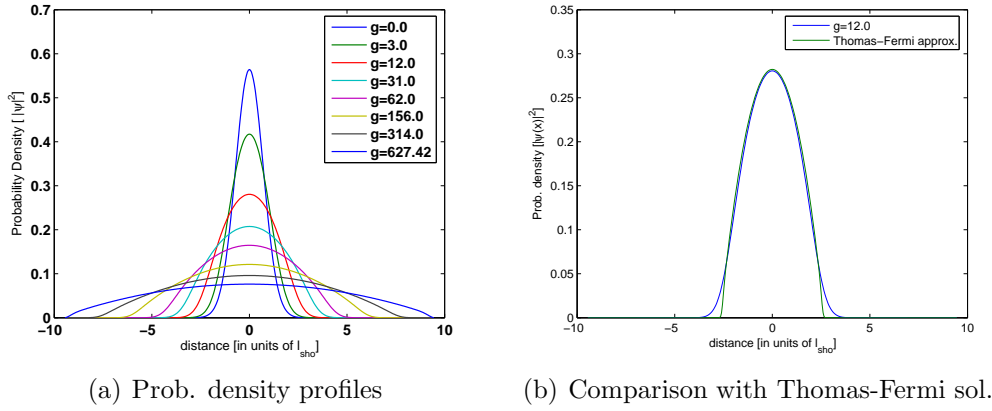


Figure 4.1:

in the absence of non-linear interactions,

$$\psi(x) \propto \exp\left(-\frac{m\omega x^2}{2\hbar}\right). \quad (4.1)$$

In figure 4.1(a), the probability density profiles have been plotted for the different values of the effective interaction strength, g , as the value of g increases the peaks descend and the condensate length along the x-axis increases. The increased inter-particle repulsive interactions causes the condensate to spread along the x-direction. Also, shown in the plot is the solution in the ideal gas limit when the gas is so dilute that the interactions between the atoms have been neglected.

Figure 4.1(b), shows the comparison of the density profile for $g = 12.0$ with the Thomas-Fermi approximation. A comparative study of the two curves reveals that the Thomas-Fermi solution is a very good representation of the wavefunction in the center of the trap, but it fails to remain so at the edges of the condensate, where the density is so low that the kinetic energy term in the GP equation can not be neglected.

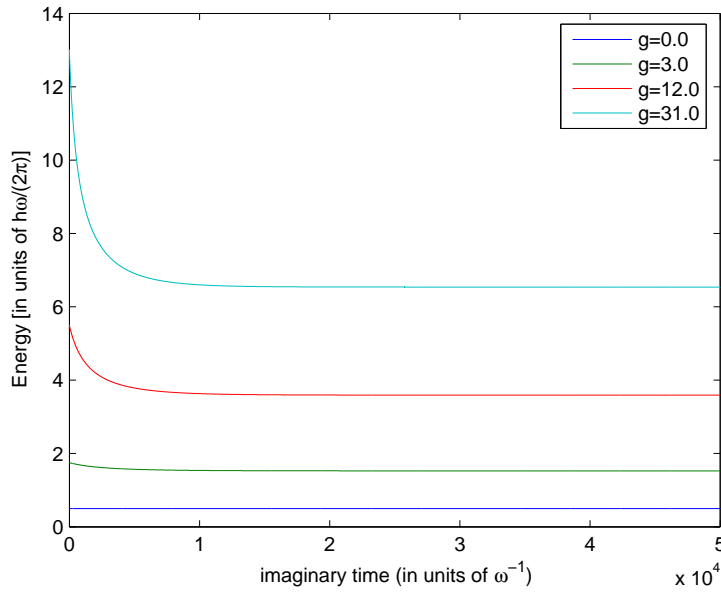


Figure 4.2:

The figure 4.2, shows the energy curves obtained for the different values of the one-dimensional effective interaction strength as a function of imaginary time. The curves show a perfect convergence after a large number of imaginary time steps, which is in accord with the imaginary time propagation algorithm, section (2.8.2). The convergence of the curves shows that the ground state has been reached.

4.1.2 Optical lattice

After studying the condensate properties in a harmonic confinement an optical lattice potential was superposed on it.

Variation of the effective interaction strength

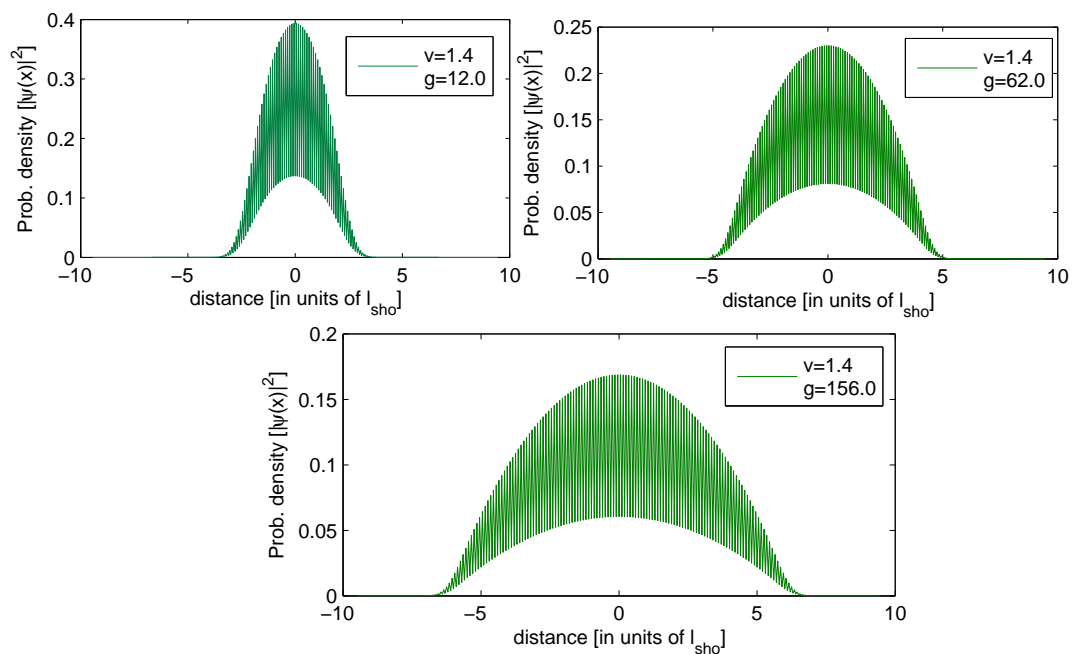


Figure 4.3:

The figure (4.3), shows the plots of density profile for different values of the one-dimensional interaction strength at a constant value of optical lattice potential, $v_{ol} = 1.4E_R$. v_{ol} has been expressed in terms of the recoil energy $E_R = \frac{\hbar^2\pi^2}{2md^2}$, where d is the dimensionless lattice constant. As in the case of one-dimensional condensate without any optical lattice here too the condensate spreads along the x-axis due to the repulsive interaction between the condensate atoms with increasing value of the effective interaction strength. Also, the periodicity of the lattice is getting reflected in the condensate density profile, which is showing a periodic increase and decrease in the probability density.

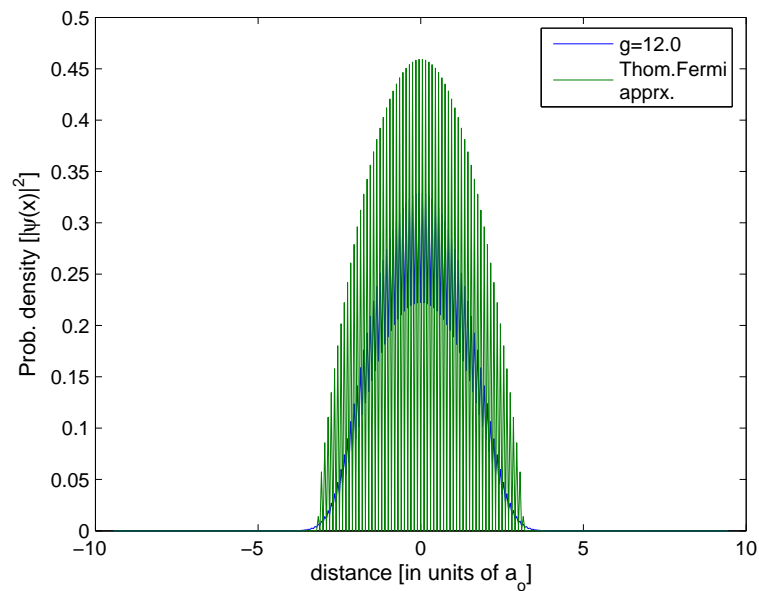
Comparison with Thomas-Fermi approximation

Figure 4.4:

Here, in figure (4.4), a comparative plot of the density profile for $g = 12.0$ with Thomas-Fermi solution has been given. The behavior is as expected, near the edges the exact numerical solution deviates from the Thomas-Fermi approximation.

Variation of optical lattice potential strength

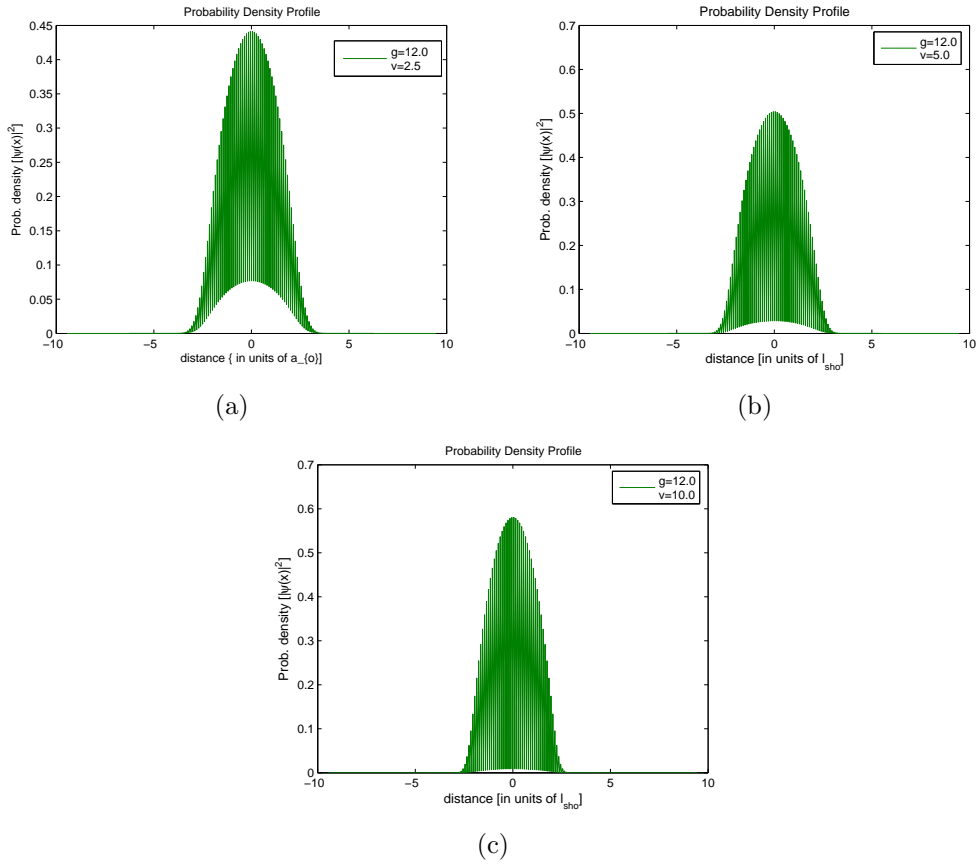


Figure 4.5:

The figure (4.5), shows the density profiles obtained for the different values of the optical lattice potential. As the potential strength is increased the condensate gets more and more localized at the potential minimas in the optical lattice, which can be approximated to small harmonic traps placed periodically along the length of the lattice.

4.2 Vortex formation in a rotating box

In this section the results following the discussion in the section (3.2.4) on the vortex formation in a rotating box have been presented. Again, the ground state solution has been computed following the ITP algorithm.

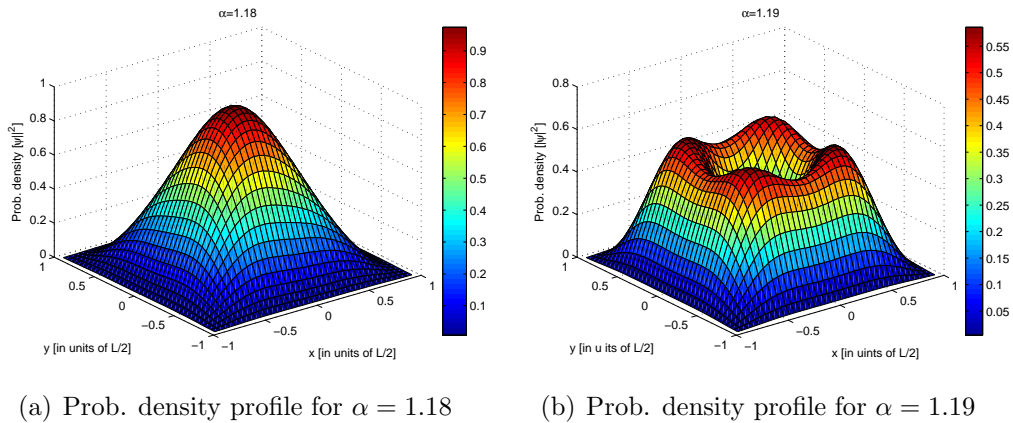


Figure 4.6:

Initially for the rotation there is no vortex formation in the density profile, but as the rotational frequency is increased, at around $\alpha = 1.19$ a depletion in the density profile occurs at the center. A phase plot for the vortex state as

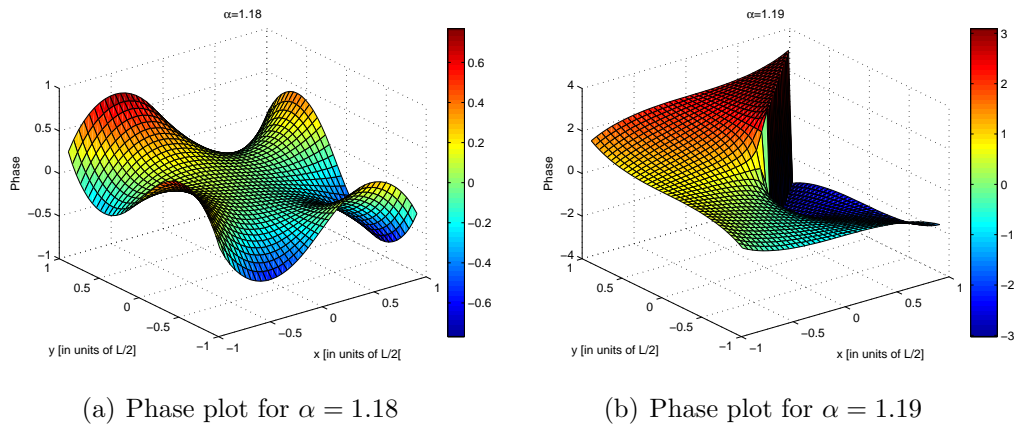


Figure 4.7:

in figure 4.7(b) shows a change of phase of 2π in one complete rotation around the hole at the center in the density profile, which signals the presence of a vortex.

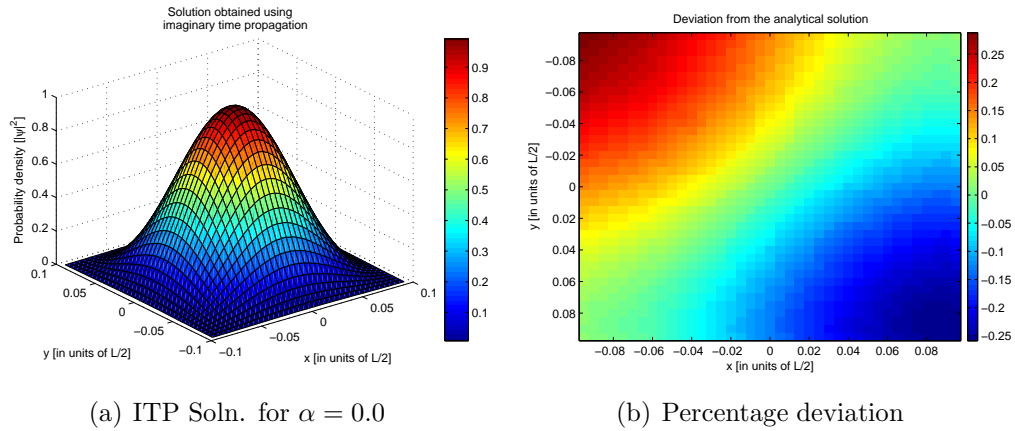


Figure 4.8:

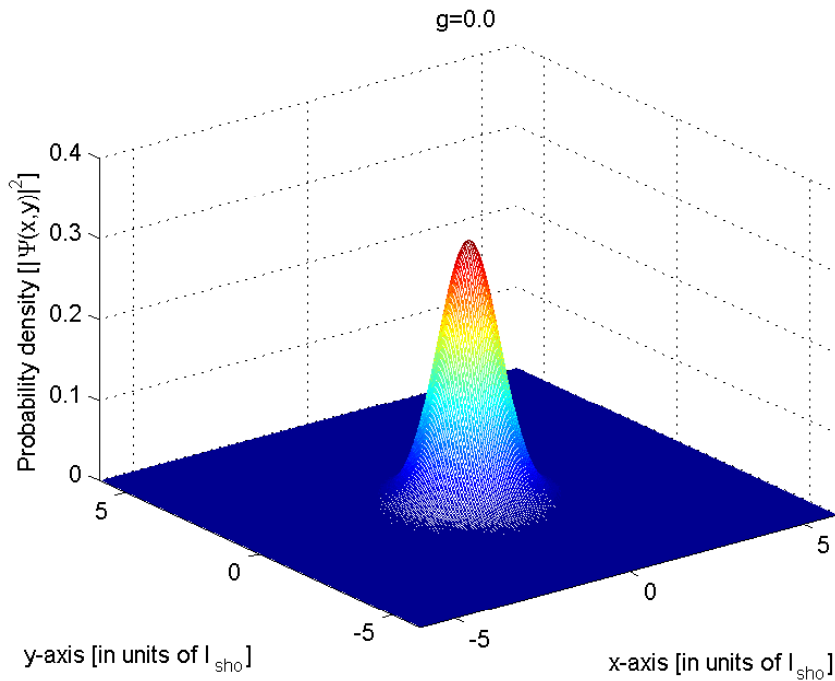
The figure (4.8) shows the percentage deviation of the ITP solution from its analytical counterpart when the box is not rotating. The observed maximum percentage deviation was found to be 0.25 percent, which is quite acceptable.

4.3 Two-dimensional Bose-Einstein condensation

At the next level of complexity is the solution of the Gross-Pitaevskii equation in two-dimensions. In the present section, first of all the ground state solution of the GP equation for the harmonic confinement and the optical lattice confinement is given.

4.3.1 Harmonic confinement

Once again, as in the case of a 1D condensate following the discussions of the sections (2.2.1), and (2.7.1) the ground state solution of the GP equation describing a two-dimensional condensate has been computed using the ITP algorithm, section (2.8.2).



(a) The ideal gas limit

Figure 4.9:

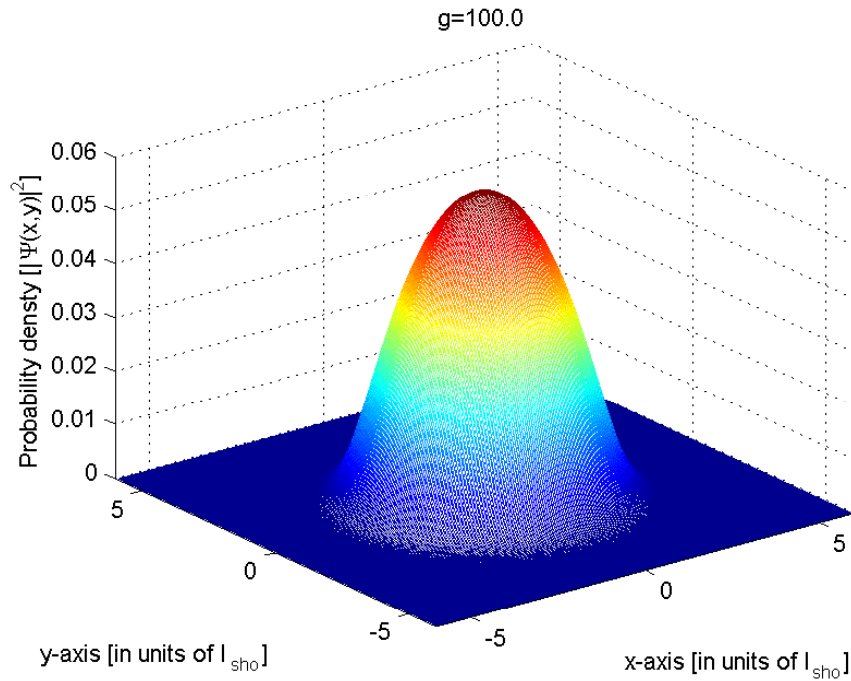
(a) Density profile for $g=100.0$

Figure 4.10:

The figure 4.9(a) shows the density profile of the condensate in the ideal gas limit, section (2.7.2). In an extremely dilute condensate the interaction between the condensate atoms may be neglected, and this yields a density profile for the condensate similar to the one obtained for a single particle in 2D harmonic oscillator potential.

Figure 4.10(a) shows that when the effective interaction strength is increased the condensate peak descends and the repulsive interactions among the condensate causes it to increase in length radially (in the x-y plane).

4.3.2 Stationary optical lattice

Here, the ground state solution of the GP equation describing the two-dimension condensate in a stationary optical lattice potential has been presented. The figure 4.11 (a) to (f), shows the effect of slowly increasing the optical potential strength. Each plot shows the projection of the density profile on the x-y plane. With the increase in the optical lattice potential strength the condensate density profile shows peaks at sites of lower potential felt by the condensate atoms, a effect which becomes more apparent with increase in the strength of the former. Thus, the condensate density profile mimics the oscillatory pattern of the imposed optical lattice in the harmonic trap.

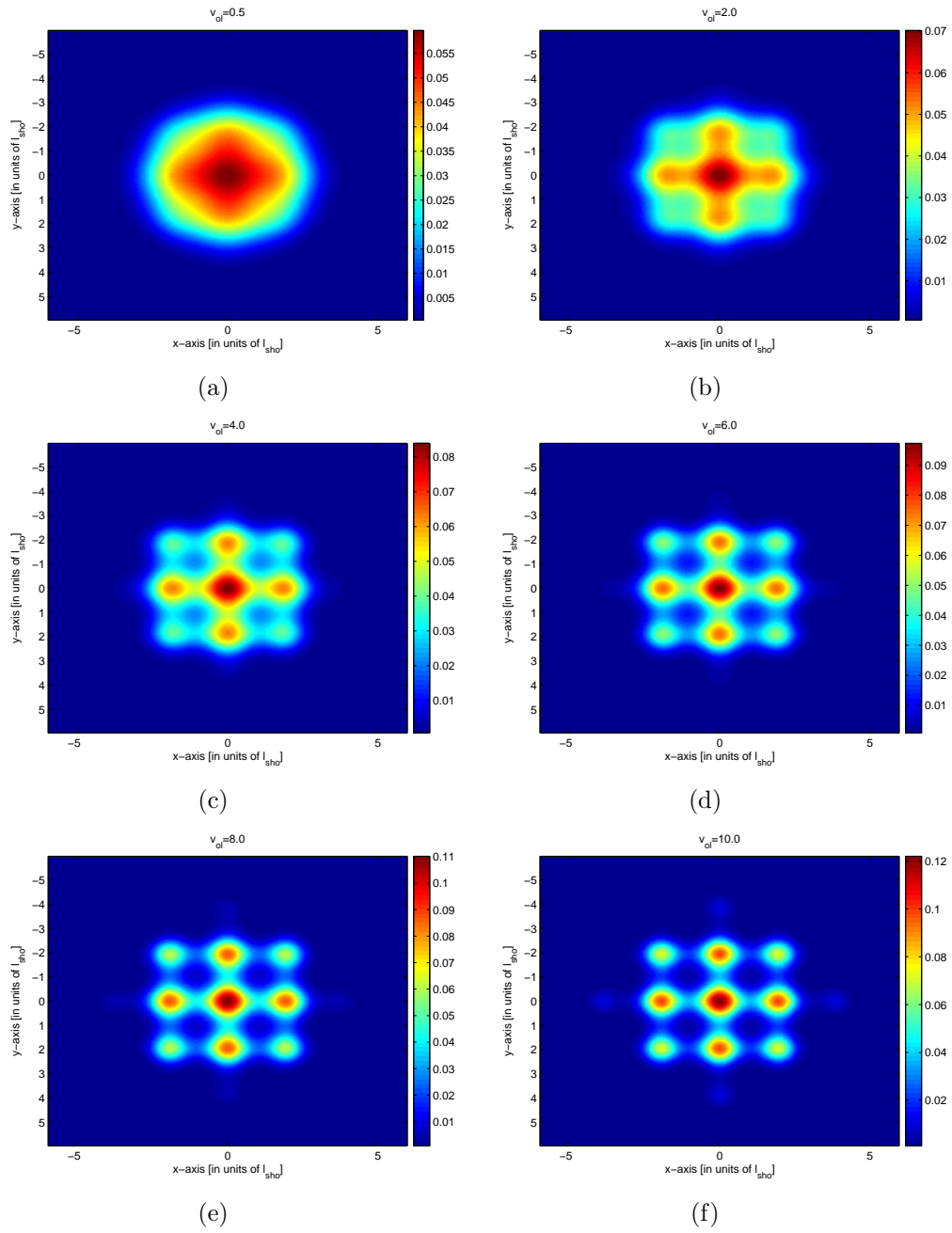


Figure 4.11: Density profiles (projection on the x-y plane)

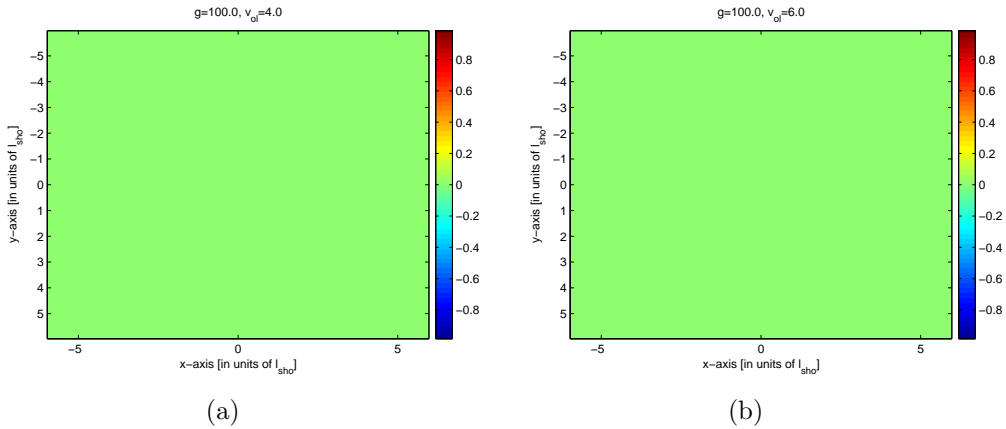


Figure 4.12: projection on the x-y plane

Figure (4.12) shows the phase distribution for the two-dimensional condensate in a stationary optical lattice for two different values of $v_{ol} = 4.0$ and $v_{ol} = 6.0$. These plots indicate that the phase is uniform through out and there is no singularity at any point in the phase.

4.4 Rotating optical lattice

In this section finally the case of rotating optical lattice has been considered. The discussion of the section (3.3) requires the solution of the GP equation describing a two-dimensional condensate present in a ground state confined in a harmonic trap when a rotating optical lattice potential is switched on. Here too, the ground state solution has been obtained numerically using the ITP algorithm. Since, a rotating optical lattice combines the effect of both the rotation and the optical lattice, so a two stage study was done. First the lattice potential was kept constant and the rotational frequency of the lattice was varied in small steps and the resulting were analyzed. Secondly, the rotational frequency was kept constant and the optical lattice potential strength was varied to study the effects it produces on the ground state properties of the condensate.

4.4.1 Variation of rotation frequency

The ground state solutions obtained, have been presented in the figure 4.13 (a) to (d). A comparative study of the probability density plots shows that with the increase in the rotation frequency the condensate atoms redistribute themselves on the x-y plane, covering many more maximas and minimas of the optical lattice, under the combined effect of the repulsive interactions between the condensate atoms and the centrifugal force due the rotational motion. The central region has the highest probability density since there both the harmonic trap and the optical lattice minima coincided, at least for the rotation frequencies investigated.

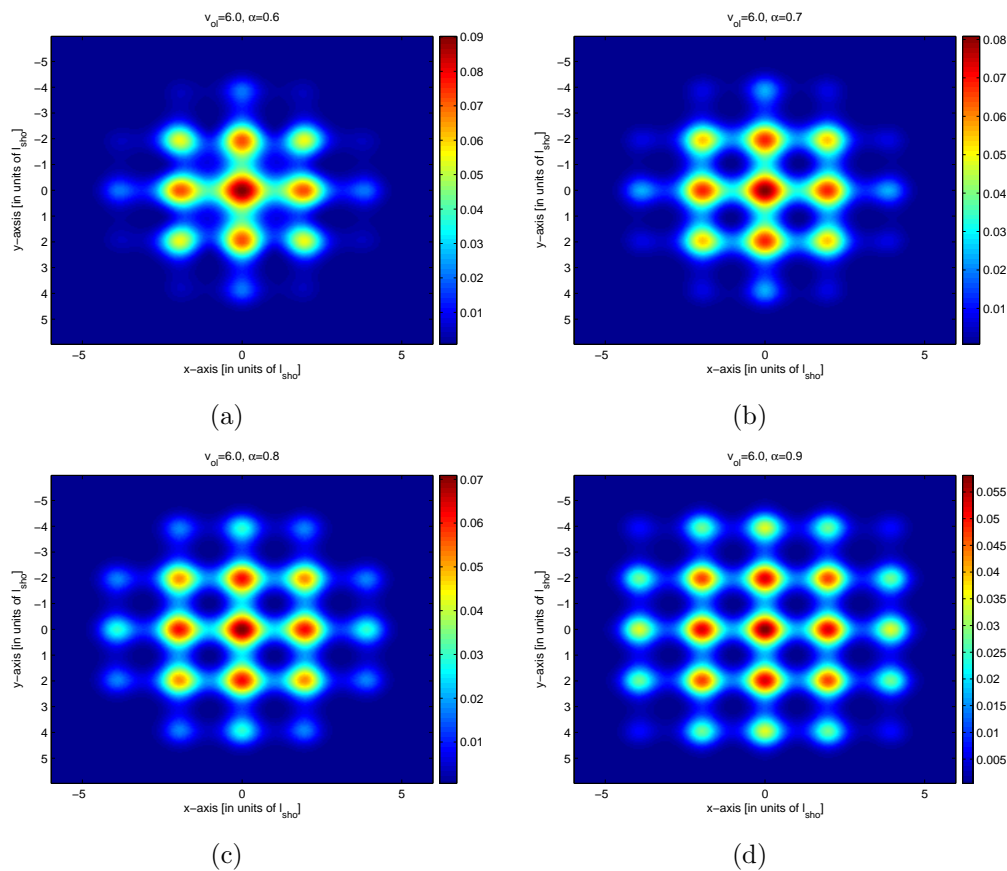


Figure 4.13: Probability density profiles (projection on the x-y plane)

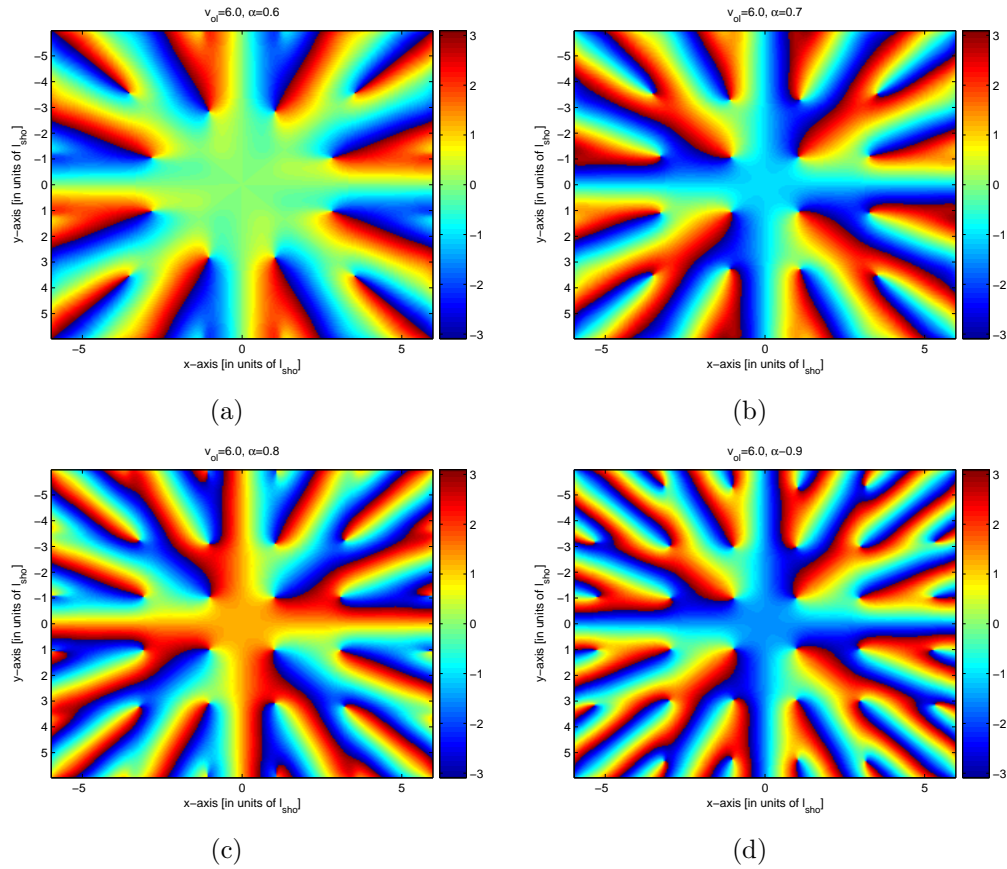


Figure 4.14: Phase distributions

A comparative study of the phase plots, figure 4.14 (a) to (d), for the increasing values of the rotation frequency at a constant value of $v_{ol} = 6.0$ shows that the number of vortices in the condensate increases with it. The presence of a vortex may be detected by observing the phase change, indicated by the color change from blue ($-\pi$) to red (π) in a given region of the plot, of 2π signalling a vortex.

4.4.2 Variation of the optical lattice potential strength

A study of the plots from (a) to (d) in the figure (4.15), at constant value of $\alpha = 0.7$ shows that with the increasing value of the optical lattice strength, the condensate atoms redistribute themselves over a large area of the optical lattice. When seen along the x-(or y) axis at a constant y (or x) the condensate density profile shows an oscillatory behavior, reflecting effects of the periodic behavior of the optical lattice on the condensate. The optical lattice potential minimas can be approximated to small potential wells periodically arranged over the entire horizontal plane.

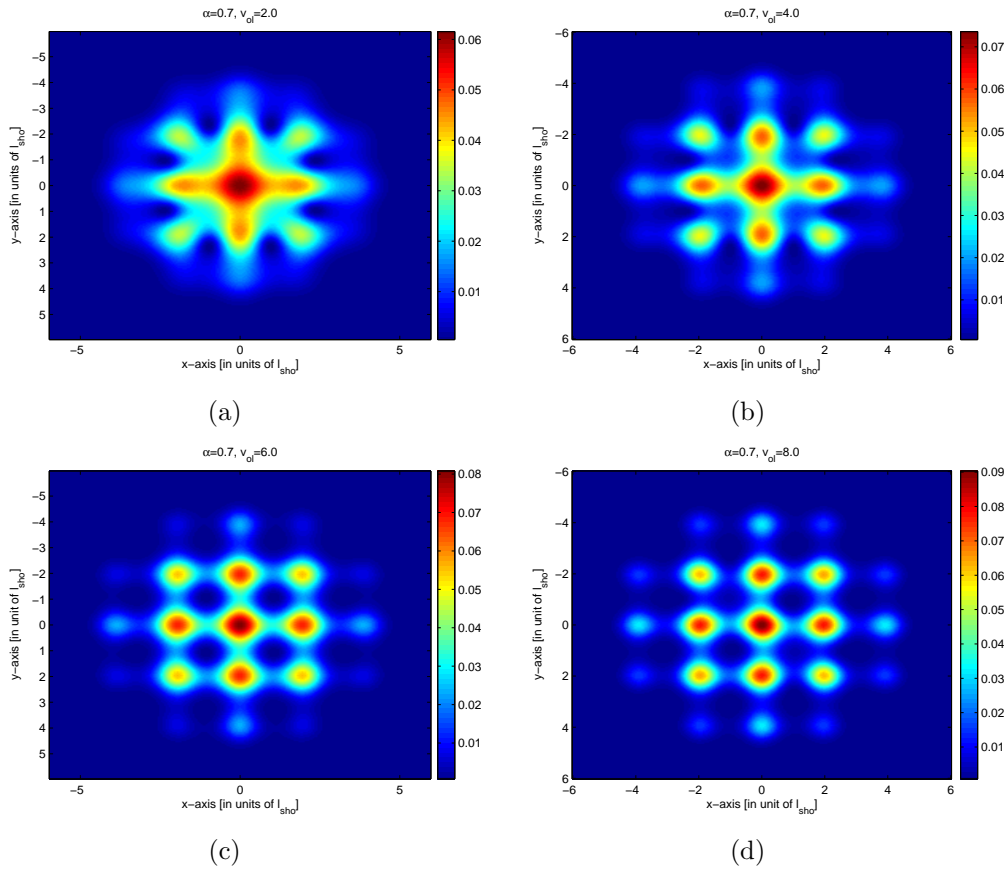


Figure 4.15: Density profiles, (projection on the x-y plane)

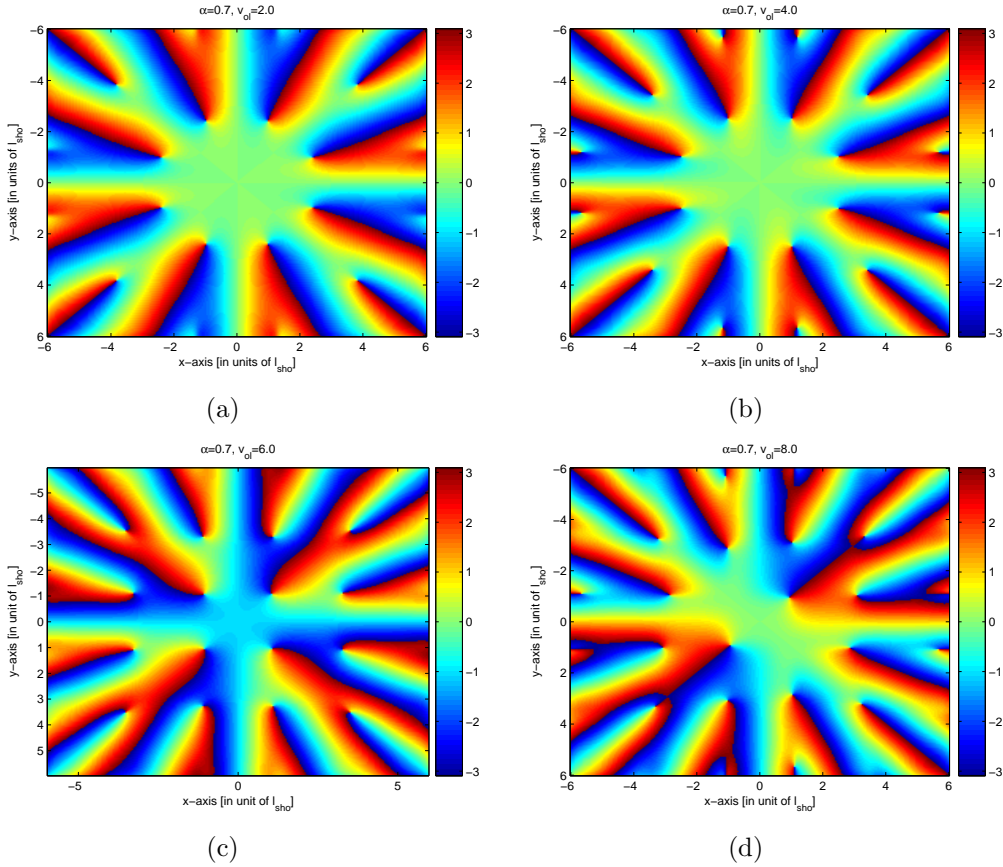


Figure 4.16: Phase distribution

As can be inferred from the phase plots (a) to (d) in the figure (4.16) for an increasing values of the optical lattice potential strength at a constant rotation frequency of $\alpha = 0.7$ the number of vortices in the condensate increases. This means that optical lattice potential is helping in the formation of vortices.

Another study which possibly could have been done, was to observe for each optical lattice potential strength the rotation frequency at which vortex is nucleated into the system and then this could be compared to the values of rotation frequency without the optical lattice at which the vortex is nucleated into the system. This would have had made the role of the optical lattice potential clearer on the vortex nucleation in the system. But, unfortunately, the computational time for the each case is very large so such an analysis could not be done.

Chapter 5

Conclusions

The present study has been done to explore the properties of a Bose-Einstein condensate confined in a rotating optical lattice. The entire study has been carried out under the mean-field approximation for a dilute weakly interacting Bose-Einstein condensate atoms. In this regime, the ground state properties were investigated using the Gross-Pitaevskii equation, and the interactions between condensate atoms gave rise to a non-linearity in the system which tilted the balance in the favor of numerical methods over the analytical ones (which are not possible except under few special circumstances).

While working on the problem an approach of dividing the complex ones into the smaller and simpler parts was adopted. So to begin with, the ground state properties of a one-dimensional Bose-Einstein condensate were studied in the harmonic and optical lattice confinement to observe the role of interactions and what extra effect an optical lattice might introduce. After studying the one-dimensional condensate in detail, the case of a two-dimensional condensate was taken up. Here too, the role of interactions and the two-dimensional optical lattice were looked for. Finally, the case of a rotating optical lattice was considered. The study of the ground state properties has revealed that an optical lattice confinement assists in the vortex formation in the condensate, apart from introducing its periodic character in the condensate density profile.

The study could have been extended further to explore the band-structure properties for the condensate in a rotating optical lattice, and also to study the effects non-linearity introduces in the system. But to do so a heavy computational work is required which has limited the scope of extension of the present work in this direction.

Bibliography

- [1] R.K. Pathria, *Statistical Mechanics*, Pergamon Press, (reprint) 1985.
- [2] C.A. Sackett, R.G. Hulet, *Science Spectra Issue* 21, 2000.
- [3] M. H. Anderson, J. R. Ensher, M. R. Matthews, C. E. Wieman, E. A. Cornell, *Science, New Series*, Vol. 269, No. 5221, (Jul. 14, 1995), pp. 198-201.
- [4] C. J. Pethick, H. Smith, *Bose-Einstein condensation in dilute gases*, Cambridge University Press, 2001.
- [5] K. Burnett, M. Edwards, C. Clark, *Physics Today*, December 1999.
- [6] Wolfgang Ketterle, *Bose-Einstein Condensation: Identity Crisis for Indistinguishable particles*.
- [7] M. Griener, Simon Fölling, *Optical lattices*, *Nature*, Vol. 453, No. 5, 2008.
- [8] F. Dalfovo, S. Giorgini, L. P. Pitaevskii, S. Sandro Stringari, *Reviews of Modern Physics*, Vol. 71, No.3, April 1999.
- [9] M.L. Chiafalo, S. Succi, M. P. Tosi, *Physical Review E*, Vol. 62, No. 5, November 2000.
- [10] W. Bao, W. Tang, *Journal of Computational Physics*, 187, pp. 230-254, 2003.
- [11] I. Bloch, *Nature physics*, Vol. 1, pp. 23-30, October, 2005.
- [12] P. M. Brandon, R. Bhat, M. Krämer, M. J. Holland, arXiv:07070307v2 [cond-mat. other], 18 Oct 2007.
- [13] R. Bhat, *Bosons in rotating optical lattices*, Ph.D Thesis, University of Colorado, 2008.
- [14] L. D. Landau, E. M. Lifshitz, *Mechanics*, Pergamon Press, 1960.

- [15] S. Tung *et al.*, aXive:cond-mat/0607697v2 [cond-mat.other], 12 Dec 2006.
- [16] R. A. Williams *et al.*, Optics Express 16983, Vol. 16, No. 21, 13 Oct 2008.